BIOCHEMISTRY
including biophysical chemistry & molecular biology

Article

pubs.acs.org/biochemistry

Importance of Aspartate Residues in Balancing the Flexibility and Fine-Tuning the Catalysis of Human 3-Phosphoglycerate Kinase

Andrea Varga,*[,†] Zoltan Palmai,[‡] Zoltán Gugolya,[§] Éva Gráczer,[†] Ferenc Vonderviszt,[§] Péter Závodszky,[†] Erika Balog,[‡] and Mária Vas*[,†]

[†]Institute of Enzymology, Research Centre for Natural Sciences, Hungarian Academy of Sciences, H-1518 Budapest, P.O. Box 7, Hungary

[‡]Institute of Biophysics and Radiology, Semmelweis Medical University, H-1444 Budapest, P.O. Box 263, Hungary

[§]Bio-Nanosystems Laboratory, Research Institute of Chemical and Process Engineering, University of Pannonia, H-8201 Veszprém, P.O. Box 158, Hungary

S *Supporting Information*

ABSTRACT: The exact role of the metal ion, usually Mg^{2+}, in the catalysis of human 3-phosphoglycerate kinase, a well-studied two-domain enzyme, has not been clarified. Here we have prepared single and double alanine mutants of the potential metal-binding residues, D374 and D218. While all mutations weaken the catalytic interactions with Mg^{2+}, they surprisingly strengthen binding of both MgADP and MgATP, and the effects are even more pronounced for ADP and ATP. Thermodynamic parameters of binding indicate an increase in the binding entropy as a reason for the strengthening. In agreement with the experimental results, computer-simulated annealing calculations for the complexes of these mutants have supported the mobility of the nucleotide phosphates and, as a consequence, formation of their new interaction(s) within the active site. A similar type of mobility is suggested to be a characteristic feature of the nucleotide site of the wild-type enzyme, too, both in its inactive open conformation and in the active closed conformation. This mobility of the nucleotide phosphates that is regulated by the aspartate side chains of D218 and D374 through the complexing Mg^{2+} is suggested to be essential in enzyme function.

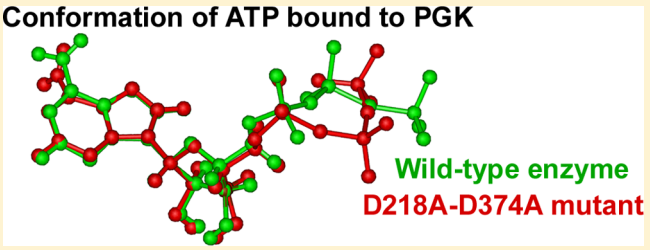

3-Phosphoglycerate kinase (PGK) is a remarkable two-domain hinge-bending enzyme, the structure−function relationship of which has been thoroughly studied over the past few decades (cf. ref 1 and references therein). At present, its functioning is rather well understood in terms of its three-dimensional structure.[2,3] PGK is a typical example of an enzyme with domain−domain interplay that is regulated by the substrates.[4−7] Relative movement of protein domains, as a manifestation of the conformational flexibility (cf. reviews in refs 1, 8, and 9), is indeed frequently involved in enzyme mechanisms.

PGK is an essential enzyme for all living organisms. It catalyzes the phospho-transfer from 1,3-bisphosphoglycerate (BPG) to MgADP and produces 3-phosphoglycerate (PG) and MgATP during the carbohydrate metabolism. In addition to its physiological role, human PGK was shown to phosphorylate L-nucleoside analogues, which are potential drugs against viral infection and cancer.[10−16]

PGK possesses two structural domains of approximately equal size,[17,18] to which the two substrates are each bound.[19,20] A large body of enzymological and structural information about PGK offers the possibility of gaining insight into the operation of its assumed molecular hinges at the atomic level and into the mechanisms of action of the two substrates (reviewed by Vas *et al.*[1]).

The C-terminal domain of PGK binds the nucleotide substrates (MgADP or MgATP),[20,21] while the N-terminal domain binds PG[19] or BPG.[2] Crystallographic data and various enzymological studies of PGKs from different sources have evidenced that domain closure, required by catalysis, takes place in the presence of both bound substrates, i.e., only in the enzyme−substrate ternary complex.[2,22−24] The high-resolution crystal structure of the catalytically competent closed conformation of human PGK (hPGK), the object of this study, provided a detailed picture of the contribution of the active site side chains to catalytic phospho-transfer.[2] Furthermore, from combined crystallographic and small-angle X-ray scattering studies, it has been hypothesized that a spring-loaded trap and release mechanism regulates the opening and closing of the domains.[3]

As for the nucleotide substrates, in their specific interactions with the protein, a complexing metal ion, usually Mg^{2+}, is also involved. It is known that in the absence of the metal ion, PGK exhibits no activity. The importance of Mg^{2+} is underlined by the fact that it is complexed to the phosphate groups of the

Received: September 3, 2012
Revised: November 20, 2012
Published: December 11, 2012

nucleotides, i.e., to the part of the substrate molecule directly involved in the kinase-catalyzed phospho-transfer reaction.[25] In general, the essential role of the metal ion in the chemistry of the phospho-transfer reactions is indeed evidenced by shielding the negative charges of the nucleotide phosphates and thereby promoting the nucleophile attack of the other substrate.[26,27] Besides the chemical role, however, the metal ion may play a further role in assisting in the domain closure together with the nucleotide substrate to which it is complexed. In this respect, the role of protein side chain(s) with which the metal ion interacts is a similarly relevant question. These questions are of general interest for the nucleotide-utilizing enzymes and still need to be clarified for PGK. Although the role of the nucleotide substrate MgATP and its phosphate chain mobility in assisting the domain closure have been hypothesized,[6,21] the importance of the potentially interacting aspartate side chains (D218 and D374 in hPGK numbering) has not been systematically tested. There is only one study of yeast PGK, in which D372 (corresponding to D374 of hPGK) was replaced with the neutral asparagine,[28] as well as a study with hPGK in which the D218N mutant has been prepared.[24] No dramatic changes have been observed in the enzyme kinetic parameters in either case.

In this work, we systematically replaced both potential metal-binding aspartates (D218 and D374) of hPGK with Ala by producing both their single and double mutants. The mutants have been characterized in enzyme kinetic and nucleotide binding experiments as well as in a computer simulation study that provided an atomic level picture of the dynamics of the interactions of the mutant proteins with the nucleotide substrates. All the data support an increase in the mobility of the nucleotide phosphate chain upon the introduction of mutations. Regulation of this mobility by the metal ion bound to the aspartates is thought to be an important element of PGK catalysis.

MATERIALS AND METHODS

Enzyme and Chemicals. Wild-type hPGK was expressed in the *Escherichia coli* BL21-CodonPlus (DE3)-RIL (Stratagene) strain, purified, and stored as described previously.[24] The mutants were prepared using a site-directed mutagenesis kit (Stratagene). Na salts of PG, ATP, and ADP were from Boehringer. The substrates, MgATP and MgADP, were formed by addition of $MgCl_2$ (Sigma) to ATP or ADP. The dissociation constants of MgATP and MgADP were taken to be 0.1 and 0.6 mM, respectively, obtained by averaging the data in the literature.[29−33]

Enzyme Activity Measurements. Enzyme activity measurements were taken using the substrates PG and MgATP.[24] The K_m values of the nucleotide MgATP were determined at a saturating concentration of the other substrate, PG. $MgCl_2$ was applied in a suitable molar excess relative to ATP to ensure the complete complexation of the latter with Mg^{2+}. The effect of Mg^{2+} concentration on enzyme activity was studied using constant concentrations of ATP (4 mM) and PG (10 mM). All measurements were taken at a low ionic strength [20 mM Tris (pH 7.5)] as described previously.[24]

Nucleotide Binding Experiments. *Thiol Reactivity.* The kinetics of the modification of the two fast reacting thiol residues of hPGK as well as mutants D218A and D374A were measured in the absence and presence of different concentrations of nucleotides. Apparent first-order rate constants were determined at a constant concentration of the Nbs_2 reagent, monitoring the increase in the absorbance of the cleaved Nbs_2 at 412 nm. Then, the second-order rate constant was calculated (ε = 14150 M^{-1} cm^{-1}) and plotted as a function of nucleotide concentration (see Figure 1). The experiments were conducted in 50 mM Tris-HCl buffer (pH 7.5) containing 1 mM EDTA at 20 °C. The binding curves were fit using eq 1.

$$k = k_{max} - \frac{(k_{max} - k_{min})[N]}{K_d + [N]} \quad (1)$$

where k_{max}, k_{min}, and k are the rate constants of thiol modification in the absence of the nucleotide, at an infinite concentration of the nucleotide, and at an intermediate concentration of the nucleotide applied in the experiment, respectively, and [N] is the free nucleotide concentration in the reaction mixture (it can be replaced by the total concentration as the enzyme-bound nucleotide is negligible under the experimental conditions).

ITC Experiments. The measurements were taken with a MicroCal VP-ITC type microcalorimeter (MicroCal Inc.) in 50 mM Tris buffer (pH 7.5) containing 1 mM EDTA and 1 mM β-mercaptoethanol at 20 °C. A typical titration experiment consisted of consecutive injections of 5 μL of the titrating ligand (in approximately 60 steps), at 3 min intervals, into the protein solution in the cell with a volume of 1.42 mL. The titration data were corrected for the small heat changes observed in control titrations of ligands into the buffer. The data were analyzed by assuming a 1:1 binding stoichiometry using MicroCal Origin 5.0.

PGK-Bound ANS Fluorescence. Changes in the PGK-bound ANS fluorescence were measured using 3 μM hPGK and 150 μM ANS in the absence and presence of nucleotides with excitation at 350 nm and emission at 478 nm in a SPEX Fluoromax-3 spectrofluorometer equipped with a Peltier (Edison, NJ) thermostat. The measurements were taken in 50 mM Tris-HCl and 1 mM EDTA (pH 7.5) at 20 °C. From the measured fluorescence intensity ($F_{measured}$) at a constant wavelength at various concentrations of a given ligand ([N]), the values of K_d were obtained by fitting the experimental points to eq 2.

$$F_{measured} = F_{max} - \frac{(F_{max} - F_{min})[N]}{K_d + [N]} \quad (2)$$

Computer Modeling. The simulated annealing method[34,35] was applied in the conformational exploration of different hPGK mutants.

The starting structure for the wild-type hPGK·MgADP complex (open conformation) was taken from Protein Data Bank (PDB) entry 2XE7;[3] the position of the Mg^{2+} ion was modeled into this structure on the basis of the MgADP-bound structure (PDB entry 1PHP) of *Bacillus stearothermophilus* PGK.[20]

Because there are no existing structures for the wild-type hPGK·ATP and hPGK·MgATP complexes (open conformations), to carefully take the nucleotide binding pocket into account, we constructed the structures of these complexes from the corresponding crystal structures of pig muscle PGK (PDB entries 1VJC and 1VJD, respectively) using InsightII. These crystal structures contain either ATP or MgATP, and their sequences are 97% identical with that of hPGK having conserved residues at the binding site. Therefore, a backbone alignment of the different residues and replacement of them with the amino acid library of InsightII were performed. We

note that the root-mean-square deviation between the binding pocket of the nucleotide constructed in this way and the binding pocket of PDB entry 2XE7 is 1.39 Å, showing a very similar conformation.

The starting structure of the hPGK·MgATP·PG complex (closed conformation) was taken from PDB entry 2WZB. The crystal structure contains ADP, PG, Mg, and the transition state analogue, MgF_3. The coordinates of MgF_3 were used to construct the γ-phosphate of the ATP molecule. The optimal conformation of ATP phosphates and their positioning in the active site were determined by an energy minimization procedure as described below. The calculations were performed on the wild-type, D218A and D374A single mutants, and D218A/D374A double mutant of each system. The mutant structures were prepared by the simple replacement of the given residue with alanine in the crystal structure and then subjected to energy minimization.

The simulations were performed using CHARMM[36] version 31b2 with the all-atom-27 protein force field. Positions for hydrogen atoms were generated by the HBUILD routine of CHARMM. To eliminate initial strains, all systems were energy-minimized in implicit water (ε = 78) using a distance-dependent dielectric constant. Van der Waals interactions were reduced to zero by "switch" truncation operating between 10.0 and 12.0 Å. Harmonic constraints were applied to heavy atoms to achieve smooth minimization. After every 500 steps of the steepest descent algorithm at values of 10, 1, and 0.1 kcal mol^{-1} $Å^{-2}$, followed by 200 steps of the conjugate gradient with a force constant of 0.1 kcal mol^{-1} $Å^{-2}$, the process was continued by an unconstrained minimization for 100 steps of steepest descent followed by 1000 steps of the conjugate gradient method. Thereafter, each energy-minimized system was subjected to the simulated annealing protocol. The heating of the systems was performed from 0 to 1000 K in 1 ps, and then they were cooled from 1000 to 300 K in 75 ps. The time step was set to 1 fs. The applied energy parameters were similar to those of the energy minimization. During the protocol, backbone atoms of the protein were constrained to their initial position by applying a force constant of 80 kcal mol^{-1} $Å^{-2}$. To explore the conformational map of the ligands, but to avoid artifacts such as the ligand leaving the binding pocket, a distance constraint with the same force constant was applied to the adenine and ribose part of ADP/ATP, to the phosphate group of PG, to Mg^{2+}, and to their known amino acid side chain contacts,[2,37] leaving the phosphate groups of the nucleotide and the carboxyl group of PG free to move.

Twenty different simulated annealing runs with different random number seeds were conducted for all systems. Each cooled conformation was energy-minimized as described above. To follow the conformational change of the nucleotides mapped by the simulation annealing runs, the displacements of the main chain nucleotide atoms were calculated with respect to the original energy-minimized positions. To characterize the modes of binding of the phosphate chain of the nucleotide detected by simulated annealing, the distances of the phosphate group atoms and their known amino acid contacts are calculated for each conformation.

RESULTS AND DISCUSSION

Mutations of D218 or D374 Strengthen the Binding of Mg-Free Nucleotides to PGK via the Increasing Flexibility of Binding. Potential Mg-binding site mutants D218A, D374A, and double mutant D218A/D374A were characterized in nucleotide binding studies. First, we studied binding of the Mg-free nucleotides, ADP and ATP, using three different methods. These are important control experiments, because the Mg-free nucleotides are not substrates for PGK but provide the basis for comparison to the behavior of their Mg-complexed counterparts. Typical experimental binding curves for Mg-free ADP obtained by the thiol reactivity method are illustrated in Figure 1. Here, binding of ADP to D218A and

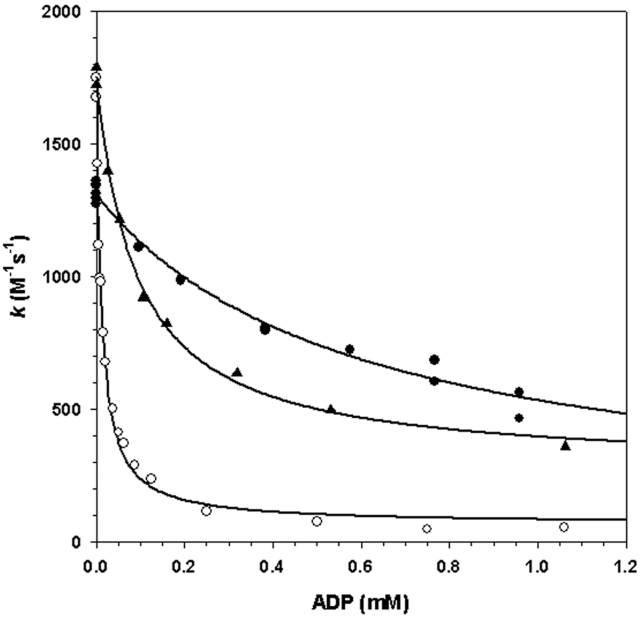

Figure 1. ADP binding to wild-type D218A and D374A mutant PGKs in the absence of Mg^{2+}. The reactivity of the accessible thiol groups of 8 μM wild-type (●), D218A (○), and D374A (▲) PGK was measured at different ADP concentrations. Curve fitting was conducted using eq 1 of Materials and Methods. The k_{max} values were 1310 ± 20, 1751 ± 22, and 1681 ± 30 M^{-1} s^{-1} for the wild-type, D218A, and D374A, respectively. K_d values are summarized in Table 1.

D374A mutants is compared with that of wild-type hPGK. Because according to the X-ray structures the side chains of D374 and D218 are likely not directly involved in binding of the Mg-free nucleotides, no large effect of the mutations is expected. In contrast to this expectation, however, binding of both Mg-free ADP (Figure 1) and ATP (not shown) became stronger in the following order: D218A < D374A < D218A/D374A. All the nucleotide binding data with the mutants are summarized in Table 1. The double mutant showed a synergistically stronger binding toward either ADP or ATP relative to the single mutants; namely, the initial K_d of ~300 μM of the wild-type enzyme decreased to ~1 μM. To characterize thermodynamically the strengthening effect of the mutations on the K_d values, ITC binding experiments using ATP as the ligand were performed with D374A and D218A/D374A (not shown). The data derived from these experiments are summarized in Table 2. While binding of ATP to the wild-type enzyme is entalphically driven (as we reported previously[37]), for the mutants the picture is changed completely, showing an entropically driven process. This picture suggests that the binding is accompanied by an increase in conformational flexibility. To monitor the nature and magnitude of this structural change of the enzyme–nucleotide complex, simulated annealing calculations were conducted. The results for ATP binding are illustrated by Figure 2, which clearly

Table 1. K_d Values (micromolar) for Interaction of Mg-Free ATP and ADP, MgATP, and MgADP with PGK Measured by ANS Binding, Thiol Reactivity, ITC, or Equilibrium Dialysis[a]

nucleotide	wild-type	method	D218A	method	D374A	method	D218A/D374A	method
	290 ± 30[b]	ITC						
ATP	**230 ± 30**[b]	Thiol react.	156 ± 31	ANS bind.	14.5 ± 1.5	Thiol react.	1. ± 0.5	ANS bind.
	210 ± 30[e]	Eq. dialysis			9.7 ± 3.7	ITC	1.7 ± 0.8	ITC
	270 ± 40[e]	Eq. dialysis						
ADP	**340 ± 50**[b]	Thiol react.	143 ± 28	ANS bind.	13.9 ± 1.4	Thiol react.	1.5 ± 0.5	ANS bind.
	310 ± 44	ANS bind.	82 ± 38	Thiol react.				
	590 ± 200[d]	Thiol react.						
	260 ± 30[b]	ITC						
	230 ± 30[e,f]	Eq. dialysis						
MgATP	**230 ± 50**[b]	Thiol react.	52 ± 9	ANS bind.	56 ± 10	Thiol react.	2.3 ± 0.7	ANS bind.
	306 ± 80	ANS bind.			38 ± 8	ITC	3.4 ± 0.6	ITC
	330 ± 150[c]	Thiol react.						
	60 ± 10[e,f]	Eq. dialysis						
	54 ± 10[b]	ITC						
	50 ± 10[b]	Thiol react.						
MgADP	**39 ± 14**[g]	Thiol react.	3 ± 2	ANS bind.	5 ± 2	ANS bind.	1.6 ± 0.5	ANS bind.
	54 ± 5[h]	ITC						
	9 ± 1	ANS bind.						
	29 ± 4[c]	Thiol react.						

[a]Measurements with pig PGK are indicated in bold. [b]From ref 37. [c]From ref 24. [d]From ref 14. [e]From ref 40. [f]From ref 41. [g]From ref 42. [h]From ref 7.

Table 2. Thermodynamic Parameters of Binding of ATP and MgATP to Wild-Type PGK and Its D374A and D218A/D374A Mutants[a]

nucleotide	PGK	K_d (μM)	ΔH (cal/mol)	$T\Delta S$ (cal/mol)	ΔG (cal/mol)
ATP	wild-type[b]	290 ± 30	*−3939 ± 184*	*996*	−4935
	D374A	9.7 ± 3.7	−1622 ± 13	*5098*	−6720
	D218A/D374A	1.7 ± 0.8	−2954 ± 150	*4688*	−7642
MgATP	wild-type[b]	260 ± 30	−1355 ± 280	*3302*	−4797
	D374A	38 ± 8	−2480 ± 18	*3442*	−5922
	D218A/D374A	3.4 ± 0.6	−1386 ± 26	*5939*	−7325

[a]The binding is entropically driven in all cases except for binding of ATP to wild-type PGK (see values in italics). [b]From ref 37.

supports the picture mentioned above. The conformations of ATP bound to the wild-type enzyme are well-defined and similar to the crystal structure (black) depicted also for comparison (Figure 2A−C), consistent with the low $T\Delta S$ value of binding (Table 2). However, in the case of the double mutant, one can clearly see two well-defined conformations of the nucleotide (Figure 2E) with very variable interactions with the enzyme (Figure 2F), which is consistent with the assumed flexible binding of the Mg-free nucleotide to either D374A or the double mutant. One typical example of this binding mode is shown by a simulated mode of binding of ATP to the double mutant (Figure 2D, red structure). The distance between the respective P atoms of the β-phosphate of ATP bound to the wild-type (green) and the double-mutant (red) enzyme is approximately 4 Å. Comparison of the interactions of ATP phosphates with this double mutant to those seen with the similarly simulated structure of the wild-type enzyme (green structure) clearly shows that in the absence of the aspartates the electrostatic interactions are strengthened between the negatively charged ATP phosphates and the positively charged side chains of K215 and K219. Thus, besides the increased flexibility, binding of ATP to the double mutant also can be strengthened by these electrostatic interactions. Although these latter changes are apparently not reflected in the thermodynamic binding data (Table 2), this may be due to simultaneous abolishment of some H-bonds with the other part of the nucleotide that were present in the case of the wild-type enzyme. In any case, binding of the nonsubstrate Mg-free nucleotides either to wild-type PGK or to its aspartate mutants does not represent a substrate-like binding mode.

Mutations of D218 or D374 Strengthen the Binding of MgADP and MgATP to the Open Conformation of PGK. Investigation of the binding interactions of the Mg^{2+} complexes of ADP and ATP with hPGK is more relevant, because these forms of the nucleotides are the real substrates. From structural studies, it is known that upon binding of either MgADP or MgATP to PGK in the absence of the other substrate, PG, the enzyme molecule, remains in its inactive, open conformation.[3,20,37] However, detailed analysis of the interactions of the nucleotide with protein side chains suggests that these interactions are prerequisites of the later formation of the closed active site upon additional binding of PG. Thus, it is interesting to study the possible perturbation of the interactions

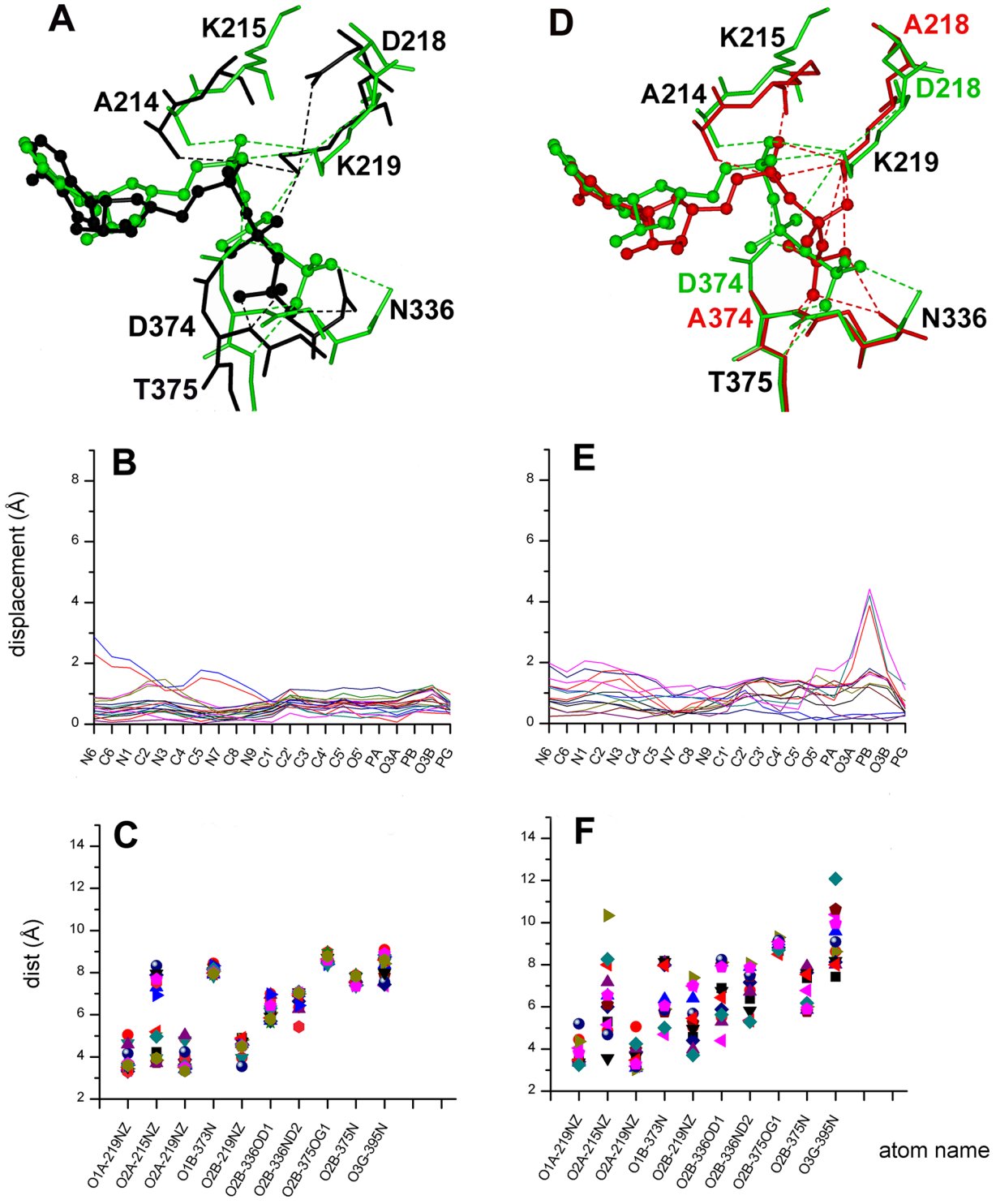

Figure 2. Modes of binding of Mg^{2+}-free ATP to the open active site of wild-type (A–C) and D218A/D374A mutant (D–F) PGKs as derived from simulated annealing computations. Representative conformations of the binding pocket of Mg^{2+}-free ATP with the side chains of the active site in wild-type PGK (green) (A and D) and in the D218A/D374A mutant (red) (D) were determined by simulated annealing calculations. As a comparison, the side chain interactions of ATP in the open crystal structure of PGK[37] are also shown (black) in panel A. The nucleotides and the side chains are depicted as balls and sticks and as sticks, respectively. Panels B and E show the displacement of the nucleotide atoms of the different simulated annealing conformations with respect to the wild-type energy-minimized crystal structure, while panels C and F show the distances from the nucleotide atoms to the atoms of binding site residues of the simulated conformations.

of MgADP and MgATP with PGK upon mutation of the two active site aspartates, D218 and D374, into the neutral alanine.

Similar to the strengthening effect of the mutations on the binding of Mg-free nucleotides, the K_d of MgATP is also decreased in the following order: wild-type, D218A, D374A, and D218A/D374A (Table 1). ITC titrations of D374A and D218A/D374A with MgATP are shown as illustrations (Figure 3). The thermodynamic parameters obtained from the ITC

dx.doi.org/10.1021/bi301194t | *Biochemistry* 2012, 51, 10197–10207

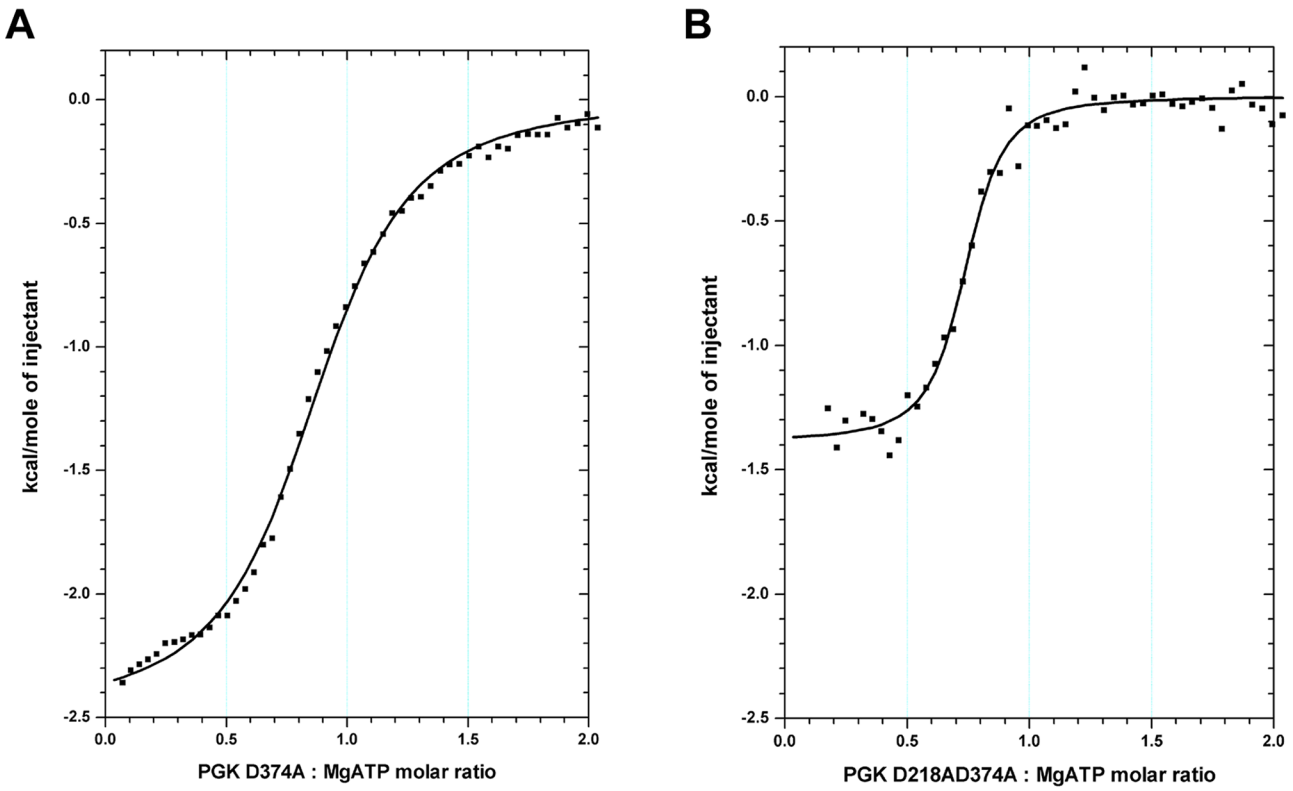

Figure 3. MgATP binding curves of mutants D374A (A) and D218A/D374A (B) PGKs measured by isothermal titration calorimetry. (A) Binding of 8 mM ATP to 0.8 mM D374A PGK in the presence of 12 mM $MgCl_2$ was measured. (B) D218A/D374A PGK (0.4 mM) was titrated with 4 mM ATP in the presence of 20 mM $MgCl_2$. The number of binding sites (N) was 0.80 and 0.75, respectively, per mole of enzyme, possibly because of some errors in the protein concentration and/or to the presence of partially inactive enzyme molecules present in the highly concentrated protein solutions. The derived K_d values as well as the thermodynamic parameters of nucleotide binding are summarized in Table 2.

experiments are compared with the values obtained previously[37] for wild-type hPGK in Table 2. It is notable that in spite of the fact that the constants for binding (K_d values) of Mg-free ATP and MgATP to the wild-type enzyme are very similar, the binding modes of the two nucleotides are completely different. ITC measurements have suggested an enthalpy-driven binding for Mg-free ATP and an entropy-driven binding for MgATP. These data have been supported by the simultaneously determined X-ray structures of ATP·hPGK and MgATP·hPGK complexes.[37] Namely, the position of the phosphate chain of ATP in the X-ray structure is very well-defined (with low crystallographic B factors): it is H-bonded to the peptide N atoms of the positively charged N-terminus of α-helix 13. On the other hand, the position of the phosphate chain of the bound MgATP is far from α-helix 13 but closer to the N-terminus of α-helix 8 (see Figure 4) and characterized by elevated B factors. The high B factor values indicate a considerable extent of flexibility of the MgATP phosphates as bound to wild-type hPGK, fully consistent with the high binding entropy (Table 2). It was hypothesized that this movement of the MgATP phosphates between the N-termini of helices 8 and 13 facilitates movement of these two helices closer to each other during the conformational transition from the open to the active closed state (cf. Figure 4), where the N-termini of these helices contribute to formation of the closed active site.

These mutations had a somewhat less pronounced strengthening effect on binding of MgATP than that shown above for Mg-free ATP, possibly because of the inherent flexibility of the MgATP phosphates as bound to the wild-type

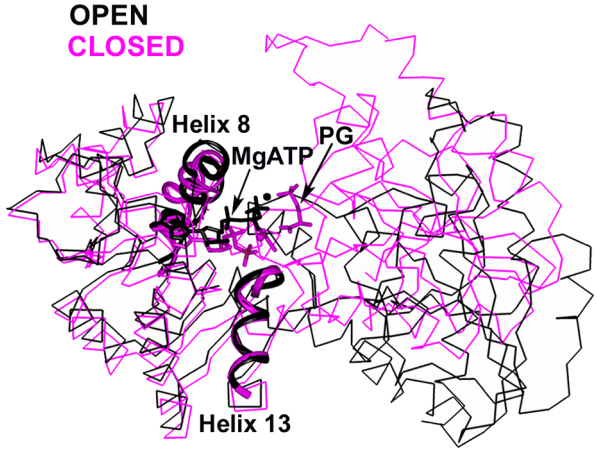

Figure 4. Comparison of the open and closed PGK conformations with respect to the mobilities of the phosphates of MgATP and the movement of helix 8 relative to helix 13. Cα traces of the open conformation (PDB entry 1VJD) of the complex of PGK with MgATP (black) and of the closed conformation (PDB entry 2WZB) of the complex of PGK with MgADP, PG, and the transition state analogue, MgF_3 (purple), are superimposed according to the inner β-strands of the C-terminal nucleotide binding domain. The bound substrates and the Mg^{2+} are represented as balls and sticks. Helices 8 and 13 are shown as ribbon diagrams of the respective colors.

enzyme. Thus, the originally entropy-driven binding of MgATP is not changed drastically upon mutation, as it is actually found (Table 2). This explanation is very well supported by the simulated annealing calculations, demonstrating, on one side,

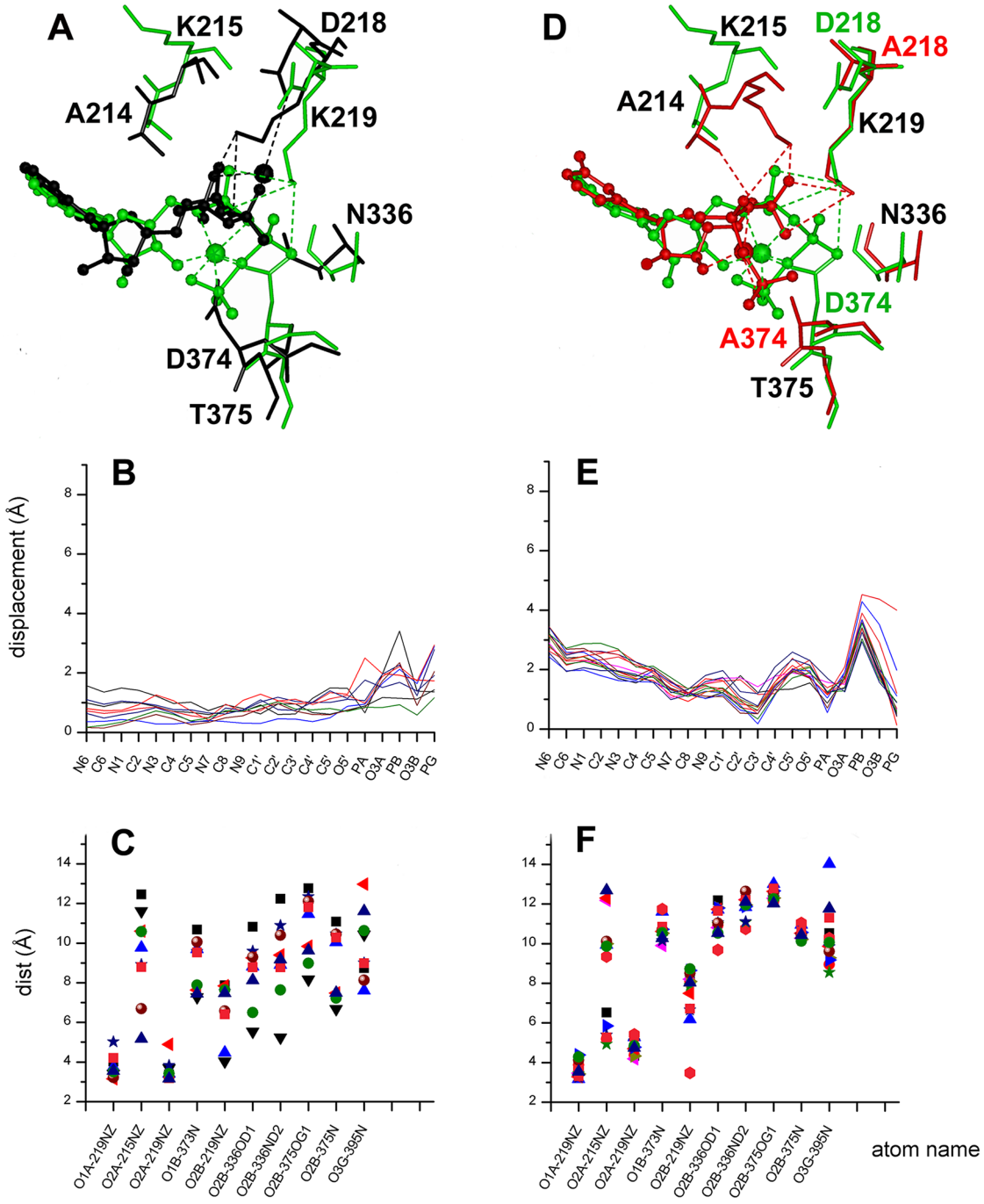

Figure 5. Modes of binding of MgATP to the open structure of wild-type (A–C) and D218A/D374A mutant (D–F) PGKs as derived from simulated annealing computation. Representative conformations of the binding pocket of MgATP with the side chains of the active site in wild-type PGK (green, A and D) and in the D218A/D374A mutant (red, D) were determined by simulated annealing calculations. As a comparison, the side chain interactions of MgATP in the open crystal structure of PGK[37] are also shown (black, A). The nucleotides and the side chains are depicted as balls and sticks and sticks, respectively. Panels B and E show the displacement of the nucleotide atoms of the different simulated annealing conformations with respect to the wild-type energy-minimized crystal structure, while panels C and F show the distances from the nucleotide atoms to the atoms of binding site residues of the simulated conformations.

the flexibility of MgATP phosphates as bound to the wild-type enzyme (Figure 5A–C) and a similarly large (4–5 Å distance) but different type of movement of the phosphate chain of MgATP bound to the D374A/D218A mutant (Figure 5D–F), on the other side.

In the case of the wild-type enzyme, both aspartates (D218 and D374) can be temporarily linked to Mg^{2+} that is otherwise linked to all three phosphates of ATP. Therefore, the aspartates may moderate the movement of ATP phosphates (note the ~5–6 Å coordinated movements of Mg^{2+}, the side chain of D374, and the γ-phosphate of ATP in Figure 5A). In the case of D218A/D374A, where these aspartates are absent, strong non-natural electrostatic interactions of the inherently flexible phosphates of MgATP may be formed with K215 and K219 (Figure 5D,F). This may also contribute to the observed strengthening of binding.

dx.doi.org/10.1021/bi301194t | *Biochemistry* 2012, 51, 10197–10207

Table 3. Kinetic Parameters of the Wild-Type and Mutants D218A, D374A, and D218A/D374A

	wild-type	D218A	D374A	D218A/D374A
k_{cat} (min^{-1})	$(1.32 \pm 0.08) \times 10^4$[a]	$(6.0 \pm 0.2) \times 10^3$	$(1.25 \pm 0.02) \times 10^4$	$(8.1 \pm 0.10) \times 10^2$
K_m (PG) (mM)	0.10 ± 0.02[a]	0.27 ± 0.02	0.12 ± 0.01	0.24 ± 0.01
K_m (MgATP) (mM)	0.11 ± 0.03[a]	0.11 ± 0.01	0.18 ± 0.02	0.20 ± 0.01
apparent K_m (Mg^{2+}) (mM)	0.53 ± 0.04	1.74 ± 0.34	3.80 ± 1.45	19.2 ± 3.8

[a]From ref 37.

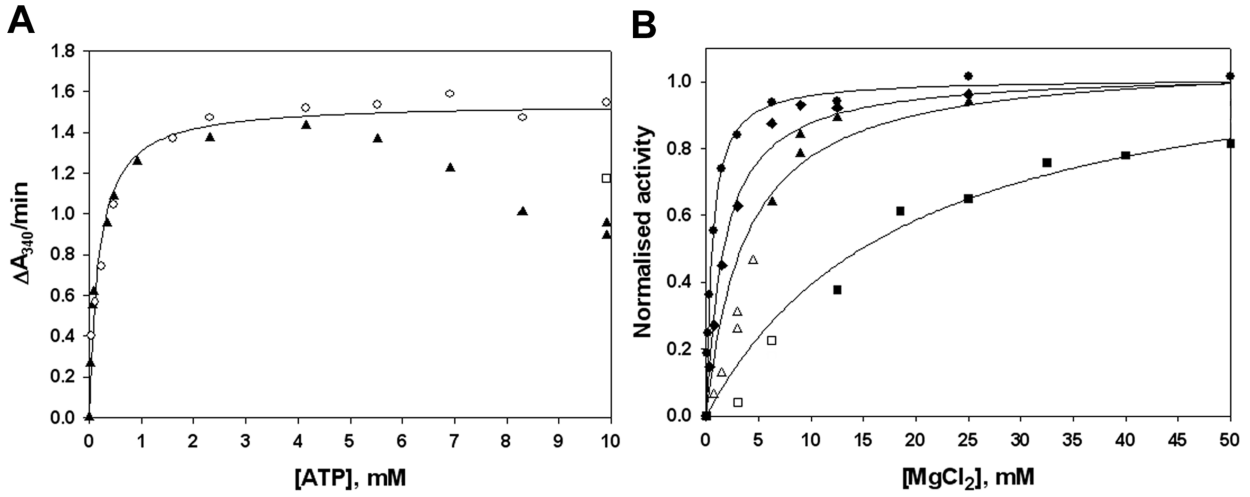

Figure 6. Dependence of enzyme activities of the investigated mutant PGKs on the concentration of Mg^{2+} ion. The activity of 19 nM D374A was measured as a function of the added ATP concentration at 10 mM PG and various constant $MgCl_2$ concentrations: 12.5 (▲), 15 (□), and 25 mM (○) (A). It is assumed that at 25 mM $MgCl_2$ all added ATP is in the form of MgATP and the K_m value obtained from the Michaelis–Menten hyperbola refers to this substrate (Table 3). Activities of 9 nM wild-type (●), 25.5 nM D218A (◆), 19 nM D374A (▲), and 206 nM D218A/D374A (■) enzyme were also measured at 4 mM ATP and 10 mM PG with increasing concentrations of added $MgCl_2$ (B). In the cases of D374A and D218A/D374A, the first few points (empty symbols) at low $MgCl_2$ concentrations are omitted from the hyperbolic fitting because of the possible inhibitory effect of ATP uncomplexed with Mg^{2+}, the concentration of which is not negligible in this $MgCl_2$ concentration range. The apparent K_m values, referring to Mg^{2+}, determined from these curves are summarized in Table 2.

Besides MgATP binding, the effect of the mutations on MgADP binding was also tested, and a similar extent of strengthening of binding has been observed (Table 1). This was not expected, especially not in the case of D374A, because the X-ray data suggest a well-defined binding of ADP through Mg^{2+} to the carboxylate side chain of D374 with low crystallographic *B* factors,[20] in agreement with the strengthening effect of Mg^{2+} on binding of ADP to wild-type PGK (Table 1). The simulated annealing calculations, however, provided a possible explanation (Figure 1 of the Supporting Information). In the case of the wild-type enzyme, the simulations resulted in a well-defined binding mode of MgADP phosphates in all the possible conformational states (Figure 1A–C of the Supporting Information). On the other hand, in the case of D218A/D374A, the other types of binding modes of the β-phosphate in which strong ionic interactions can be formed with the active site lysines are allowed (Figure 1D–F of the Supporting Information), in agreement with our experimental observations of strong MgADP binding. These ionic interactions, however, are artificial ones and do not require the contribution of Mg^{2+}, i.e., possibly nothing to do with the substrate-like binding of MgADP.

The Positioning of the Phosphate Chain of ATP via Mg^{2+} Shifts the Conformational Space toward the Productive Binding Mode of the Substrate. The binding studies with the nucleotide substrates MgADP and MgATP described above have suggested that the carboxylate side chains of both D218 and D374 are involved in Mg^{2+}-mediated substrate binding. On the other hand, no drastic changes could be observed in the main kinetic parameters (k_{cat}, $K_{m,PG}$, and $K_{m,MgATP}$) upon these mutations, at least at face value (Table 3). It has to be emphasized, however, that to obtain the normal hyperbolic substrate saturation curve, much higher concentrations of Mg^{2+} have to be applied in the enzyme activity assay mixtures of the mutants, relative to the slight molar excess over ATP that was satisfactory for the wild-type enzyme. Figure 6A shows the experiment with D374A, where increasing the concentration of $MgCl_2$ to 25 mM was required to counterbalance the activity decline observed at the lower concentration (12.5 mM) of $MgCl_2$. A further increase in the concentration of $MgCl_2$ to 40 mM did not cause any further change (not shown). In a similar experiment with the double mutant D218A/D374A, however, even addition of 100 mM $MgCl_2$ could only partially counterbalance the activity decline observed above 4 mM ATP (not shown). Thus, the K_d of 0.1 mM (averaged from the literature[29,31–33]) of the enzyme-free complex of Mg^{2+} and ATP seems to be unchanged only within the complex with the wild-type enzyme. This is in agreement with the literature data.[24,30,38,39] In cases of single and double Asp mutants, higher and higher additional concentrations of $MgCl_2$ are required to keep E·Mg·ATP complex functioning, i.e., to keep all ATP in this complex, as demonstrated with the D374A mutant in Figure 6A. The weakening effects of the Asp mutations (in the order of D218A, D374A, and D218A/D374A) on the catalytic E·Mg·ATP complex are more dramatically shown by Figure 6B when the activity was

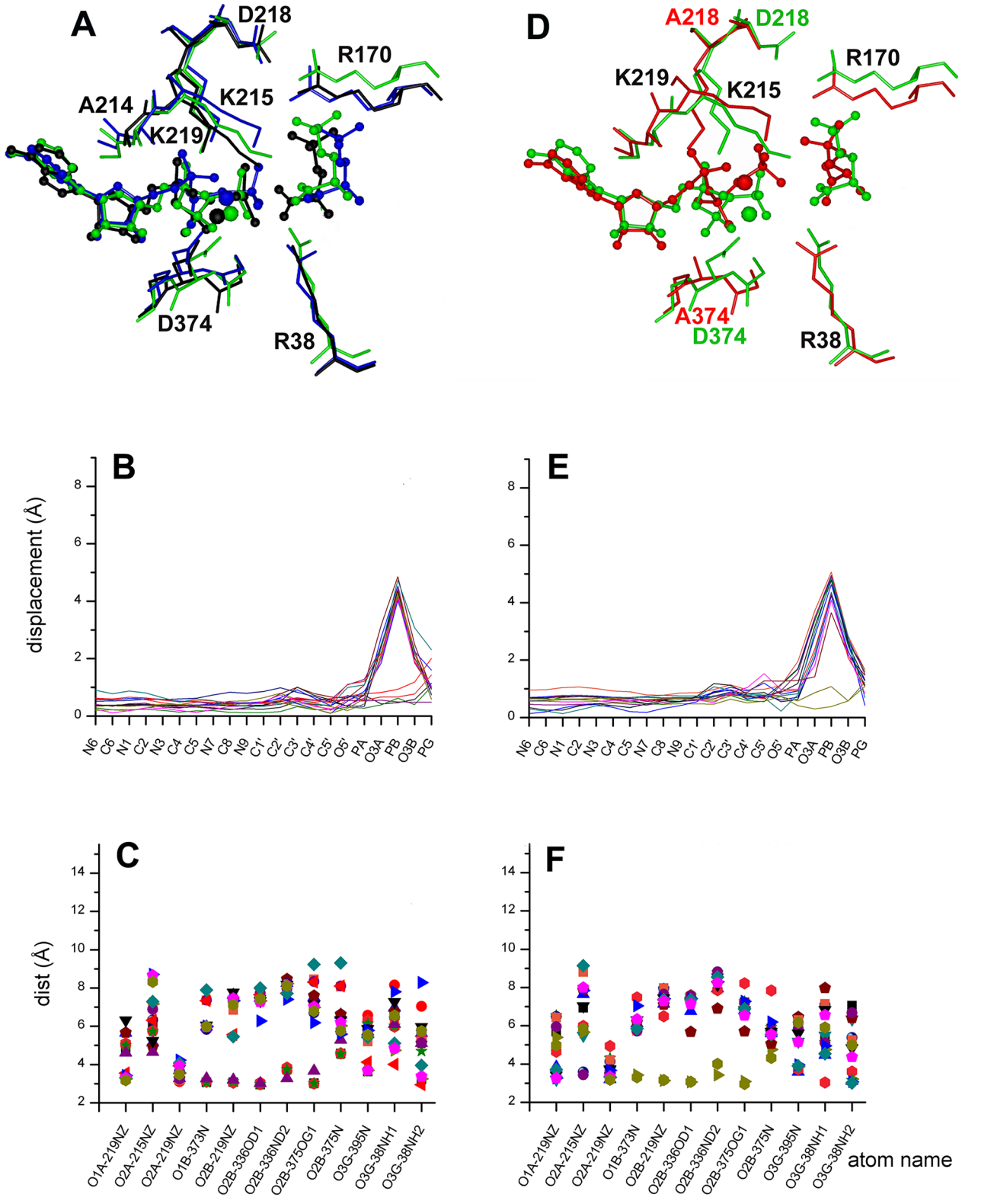

Figure 7. Modes of binding of MgATP to the closed active site of wild-type (A–C) and D218A/D374A mutant (D–F) PGKs as derived from simulated annealing computations. Representative conformations of the binding pocket of MgATP with the side chains of the closed active site in wild-type PGK (green and blue, A and D) as well as in the D218A/D374A mutant were determined by simulated annealing calculations (red, D). As a comparison, the binding mode of the nucleotide (MgADP) and the transition state analogue (MgF_3) as determined by the closed crystal structure[2] is also shown (black, A). The nucleotides and the side chains are depicted by balls and sticks and sticks, respectively. For the sake of clarity, the atomic contacts of the nucleotides with the protein are not shown. Panels B and E show the displacement of the nucleotide atoms of the different simulated annealing conformations with respect to the wild-type energy-minimized crystal structure, while panels C and F show the distances from the nucleotide atoms to the atoms of binding site residues of the simulated conformations.

dx.doi.org/10.1021/bi301194t | *Biochemistry* 2012, 51, 10197–10207

measured as a function of the added Mg^{2+} concentration. The apparent K_m values of Mg^{2+} determined from these curves are listed in Table 3. These results clearly demonstrate the importance of both D218 and D374 in the catalytic interactions with Mg^{2+}.

To gain better insight into the conformational possibilities of the substrate sites of the active enzyme as well as the effects of the aspartate mutants on it, simulated annealing calculations were conducted with the closed active conformation of PGK containing both bound substrates, MgATP and PG. The results are shown in Figure 7. At first glance, both the wild-type enzyme (Figure 7A−C) and the double mutant D128A/D374A (Figure 7D−F) behave similarly, if we consider them only at face value. Namely, some movement of the nucleotide phosphates is surprisingly allowed even within the closed state of the active site.

However, if we consider the details, significant differences can be noted between the wild-type enzyme and the mutant. The two selected representative energy-minimized wild-type structures, in comparison with the closed crystal structure of hPGK (Figure 7A), clearly show the possibility of side chain movements within the closed active site. For example, the essential K215 that normally interacts with the transferring γ-phosphate of ATP is able to move away, and therefore, this interaction is suspended. At the same time, although the position of Mg^{2+} changes very little, its interactions are weakened with both the nucleotide phosphates and the side chain of D374. These changes are accompanied by a slight opening of the active site, although it remains essentially closed. One may hypothesize that similar initial movements may assist in opening of the active site during the catalytic cycle if the enzyme acts in solution. The observed movement of Mg^{2+} would also be consistent with its assumed movement during the catalysis between the nucleotide phosphates.[26,27]

In the case of the double mutant (Figure 7D), however, in spite of the similar extent of movement of the side chain of K215, its interactions with the ATP phosphates are not suspended at all. This is in agreement with the observation that there is no effect of the present mutations on the substrate K_m values. Furthermore, in contrast to the wild-type enzyme, here Mg^{2+} moves as much as 2 Å, and its interaction with the β-phosphate of ATP is completely abolished. Thus, this simulated structure completely underlines the enzyme kinetic observations (Figure 6) of weakening of the catalytic interaction with Mg^{2+} upon mutation of D218 and D374 side chains.

In conclusion, the important role of the carboxylates of D218 and D374 in the precise positioning of Mg^{2+} toward the nucleotide phosphates in the active site of PGK during catalysis is clearly demonstrated. Furthermore, experimental and simulated annealing calculations of nucleotide binding provided deeper insight into the flexible nature of the interactions of Mg^{2+} with the nucleotides and the aspartate side chains.

■ ASSOCIATED CONTENT

Supporting Information

Modes of binding of MgADP to the open structure of wild-type (A−C) and D218A/D374A mutant (D−F) PGKs as derived from simulated annealing computations. This material is available free of charge via the Internet at http://pubs.acs.org.

■ AUTHOR INFORMATION

Corresponding Author

*Institute of Enzymology, RCNS, HAS, H-1518 Budapest, P.O. Box 7, Hungary. Telephone: 36 1 279 3152. Fax: 36 1 466 5465. E-mail: vas.maria@ttk.mta.hu (M.V.) or matkovics.varga.andrea@ttk.mta.hu (A.V.).

Funding

This work was supported by Grant OTKA (NK 77978) of the Hungarian National Research Fund. In addition, E.B. is thankful for the János Bolyai Research Scholarship provided by the Hungarian Academy of Sciences.

Notes

The authors declare no competing financial interest.

■ ACKNOWLEDGMENTS

Thanks are due to Dr. Matthew Adamson for correcting the linguistic errors throughout the text.

■ ABBREVIATIONS

hPGK, human 3-phospho-D-glycerate kinase or ATP, 3-phospho-D-glycerate 1-phosphotransferase (EC 2.7.2.3); PG, 3-phosphoglycerate; BPG, 1,3-bisphosphoglycerate.

■ REFERENCES

(1) Vas, M., Varga, A., and Gráczer, É. (2010) Insight into the mechanism of domain movements and their role in enzyme function: Example of 3-phosphoglycerate kinase. *Curr. Protein Pept. Sci. 11*, 118−147.

(2) Cliff, M. J., Bowler, M. W., Varga, A., Marston, J. P., Szabó, J., Hounslow, A. M., Baxter, N. J., Blackburn, G. M., Vas, M., and Waltho, J. P. (2010) Transition state analogue structures of human phosphoglycerate kinase establish the importance of charge balance in catalysis. *J. Am. Chem. Soc. 132*, 6507−6516.

(3) Zerrad, L., Merli, A., Schroder, G. F., Varga, A., Gráczer, É., Pernot, P., Round, A., Vas, M., and Bowler, M. W. (2011) A spring-loaded release mechanism regulates domain movement and catalysis in phosphoglycerate kinase. *J. Biol. Chem. 286*, 14040−14048.

(4) Varga, A., Flachner, B., Konarev, P., Gráczer, É., Szabó, J., Svergun, D., Závodszky, P., and Vas, M. (2006) Substrate-induced double sided H-bond network as a means of domain closure in 3-phosphoglycerate kinase. *FEBS Lett. 580*, 2698−2706.

(5) Szabó, J., Varga, A., Flachner, B., Konarev, P. V., Svergun, D. I., Závodszky, P., and Vas, M. (2008) Role of side-chains in the operation of the main molecular hinge of 3-phosphoglycerate kinase. *FEBS Lett. 582*, 1335−1340.

(6) Szabó, J., Varga, A., Flachner, B., Konarev, P. V., Svergun, D. I., Závodszky, P., and Vas, M. (2008) Communication between the Nucleotide Site and the Main Molecular Hinge of 3-Phosphoglycerate Kinase. *Biochemistry 47*, 6735−6744.

(7) Varga, A., Szabó, J., Flachner, B., Gugolya, Z., Vonderviszt, F., Závodszky, P., and Vas, M. (2009) Thermodynamic analysis of substrate induced domain closure of 3-phosphoglycerate kinase. *FEBS Lett. 583*, 3660−3664.

(8) Gerstein, M., and Echols, N. (2004) Exploring the range of protein flexibility, from a structural proteomics perspective. *Curr. Opin. Chem. Biol. 8*, 14−19.

(9) Henzler-Wildman, K. A., Lei, M., Thai, V., Kerns, S. J., Karplus, M., and Kern, D. (2007) A hierarchy of timescales in protein dynamics is linked to enzyme catalysis. *Nature 450*, 913−916.

(10) Krishnan, P., Fu, Q., Lam, W., Liou, J. Y., Dutschman, G., and Cheng, Y. C. (2002) Phosphorylation of pyrimidine deoxynucleoside analog diphosphates: Selective phosphorylation of L-nucleoside analog diphosphates by 3-phosphoglycerate kinase. *J. Biol. Chem. 277*, 5453−5459.

(11) Krishnan, P., Liou, J. Y., and Cheng, Y. C. (2002) Phosphorylation of pyrimidine L-deoxynucleoside analog diphos-

phates. Kinetics of phosphorylation and dephosphorylation of nucleoside analog diphosphates and triphosphates by 3-phosphoglycerate kinase. *J. Biol. Chem. 277*, 31593−31600.
(12) Krishnan, P., Gullen, E. A., Lam, W., Dutschman, G. E., Grill, S. P., and Cheng, Y. C. (2003) Novel role of 3-phosphoglycerate kinase, a glycolytic enzyme, in the activation of L-nucleoside analogs, a new class of anticancer and antiviral agents. *J. Biol. Chem. 278*, 36726−36732.
(13) Gallois-Montbrun, S., Faraj, A., Seclaman, E., Sommadossi, J. P., Deville-Bonne, D., and Veron, M. (2004) Broad specificity of human phosphoglycerate kinase for antiviral nucleoside analogs. *Biochem. Pharmacol. 68*, 1749−1756.
(14) Varga, A., Szabó, J., Flachner, B., Roy, B., Konarev, P., Svergun, D., Závodszky, P., Perigaud, C., Barman, T., Lionne, C., and Vas, M. (2008) Interaction of human 3-phosphoglycerate kinase with L-ADP, the mirror image of D-ADP. *Biochem. Biophys. Res. Commun. 366*, 994−1000.
(15) Gondeau, C., Chaloin, L., Lallemand, P., Roy, B., Périgaud, C., Barman, T., Varga, A., Vas, M., Lionne, C., and Arold, S. T. (2008) Molecular basis for the lack of enantioselectivity of human 3-phosphoglycerate kinase. *Nucleic Acids Res. 36*, 3620−3629.
(16) Varga, A., Chaloin, L., Sági, G., Sendula, R., Gráczer, É., Liliom, K., Závodszky, P., Lionne, C., and Vas, M. (2011) Nucleotide promiscuity of 3-phosphoglycerate kinase is in focus: Implications for the design of better anti-HIV analogues. *Mol. BioSyst. 7*, 1863−1873.
(17) Banks, R. D., Blake, C. C. F., Evans, P. R., Haser, R., Rice, D. W., Hardy, G. W., Merrett, M., and Phillips, A. W. (1979) Sequence, structure and activity of phosphoglycerate kinase: A possible hinge-bending enzyme. *Nature 279*, 773−777.
(18) Blake, C. C. F., and Rice, D. W. (1981) Phosphoglycerate kinase. *Philos. Trans. R. Soc. London, Ser. A 293*, 93−104.
(19) Harlos, K., Vas, M., and Blake, C. C. F. (1992) Crystal structure of the binary complex of pig muscle phosphoglycerate kinase and its substrate 3-phospho-D-glycerate. *Proteins 12*, 133−144.
(20) Davies, G. J., Gamblin, S. J., Littlechild, J. A., Dauter, Z., Wilson, K. S., and Watson, H. C. (1994) Structure of the ADP complex of the 3-phosphoglycerate kinase from *Bacillus stearothermophilus* at 1.65 Å. *Acta Crystallogr. D50*, 202−209.
(21) Flachner, B., Kovári, Z., Varga, A., Gugolya, Z., Vonderviszt, F., Náray-Szabó, G., and Vas, M. (2004) Role of Phosphate Chain Mobility of MgATP in Completing the 3-Phosphoglycerate Kinase Catalytic Site: Binding, Kinetic, and Crystallographic Studies with ATP and MgATP. *Biochemistry 43*, 3436−3449.
(22) Bernstein, B. E., Michels, P. A. M., and Hol, W. G. J. (1997) Synergistic effects of substrate-induced conformational changes in phosphoglycerate kinase activation. *Nature 385*, 275−278.
(23) Auerbach, G., Huber, R., Grättinger, M., Zaiss, K., Schurig, H., Jaenicke, R., and Jacob, U. (1997) Closed structure of phosphoglycerate kinase from *Thermotoga maritima* reveals the catalytic mechanism and determinants of thermal stability. *Structure 5*, 1475−1483.
(24) Flachner, B., Varga, A., Szabó, J., Barna, L., Hajdú, I., Gyimesi, G., Závodszky, P., and Vas, M. (2005) Substrate-Assisted Movement of the Catalytic Lys 215 during Domain Closure: Site-Directed Mutagenesis Studies of Human 3-Phosphoglycerate Kinase. *Biochemistry 44*, 16853−16865.
(25) Mildvan, A. S. (1981) Conformations and arrangement of substrates at active sites of ATP-utilizing enzymes. *Philos. Trans. R. Soc. London, Ser. B 293*, 65−74.
(26) Knowles, J. R. (1980) Enzyme-catalyzed phosphoryl transfer reactions. *Annu. Rev. Biochem. 49*, 877−919.
(27) Herschlag, D., and Jencks, W. P. (1987) Effect of Divalent Metal Ions on the Rate and Transition-State Structure of Phosphoryl-Transfer Reactions. *J. Am. Chem. Soc. 109*, 4665−4674.
(28) Minard, P., Bowen, D. J., Hall, L., Littlechild, J. A., and Watson, H. C. (1990) Site-directed mutagenesis of aspartic acid 372 at the ATP binding site of yeast phosphoglycerate kinase: Over-expression and characterization of the mutant enzyme. *Protein Eng. 3*, 515−521.
(29) Burton, K. (1959) Formation constants for complexes of adenosine di- or tri-phosphate with magnesium or calcium ions. *Biochem. J. 71*, 388−395.
(30) Larsson-Raznikiewicz, M. (1964) Kinetic studies on the reaction catalysed by phosphoglycerate kinase: I. The effect of Mg^{2+} and adenosine-5′-triphosphate. *Biochim. Biophys. Acta 85*, 60−68.
(31) Gupta, R. K., Gupta, P., Yashok, W. P., and Rose, Z. B. (1983) Measurement of the dissociation constant of MgATP at physiological nucleotide levels by a combination of ^{31}P NMR and optical absorbance spectroscopy. *Biochem. Biophys. Res. Commun. 117*, 210−216.
(32) Miller, C., Frey, C. M., and Stuehr, J. E. (1972) Interactions of divalent metal ions with inorganic and nucleotide phosphates. I. Thermodynamics. *J. Am. Chem. Soc. 94*, 8898−8904.
(33) Zhang, W., Truttmann, A. C., Luthi, D., and McGuigan, J. A. (1997) Apparent Mg^{2+}-adenosine 5-triphosphate dissociation constant measured with Mg^{2+} macroelectrodes under conditions pertinent to ^{31}P NMR ionized magnesium determinations. *Anal. Biochem. 251*, 246−250.
(34) Kirkpatrick, S., Gelatt, C. D., Jr., and Vecchi, M. P. (1983) Optimization by simulated annealing. *Science 220*, 671−680.
(35) Tai, K. (2004) Conformational sampling for the impatient. *Biophys. Chem. 107*, 213−220.
(36) MacKerell, A. D. J., Bashford, D., Bellott, M., Dunbrack, R. L., Evanseck, J. D., Field, M. J., Fischer, S., Gao, J., Guo, H., Ha, S., Joseph-McCarthy, D., Kuchnir, L., Kuczera, K., Lau, F. T. K., Mattos, C., Michnick, S., Ngo, T., Nguyen, D. T., Prodhom, B., Reiher, W. E., III, Roux, B., Schlenkrich, M., Smith, J., Stote, R., Straub, J., Watanabe, M., Wiorkiewicz-Kuczera, J., Yin, D., and Karplus, M. (1998) All-atom empirical potential for molecular modeling and dynamics studies of proteins. *J. Phys. Chem. B 102*, 3586−3616.
(37) Flachner, B., Kovári, Z., Varga, A., Gugolya, Z., Vonderviszt, F., Náray-Szabó, G., and Vas, M. (2004) Role of phosphate chain mobility of MgATP in completing the 3-phosphoglycerate kinase catalytic site: Binding, kinetic, and crystallographic studies with ATP and MgATP. *Biochemistry 43*, 3436−3449.
(38) Larsson-Raznikiewicz, M. (1970) The phosphoglycerate kinase reaction and its metal ion specificity. *Eur. J. Biochem. 17*, 183−192.
(39) Szilágyi, A. N., and Vas, M. (1998) Anion activation of 3-phosphoglycerate kinase requires domain closure. *Biochemistry 37*, 8551−8563.
(40) Molnár, M., and Vas, M. (1993) Mg^{2+} affects the binding of ADP but not ATP to 3-phosphoglycerate kinase. Correlation between equilibrium dialysis binding and enzyme kinetic data. *Biochem. J. 293*, 595−599.
(41) Merli, A., Szilágyi, A. N., Flachner, B., Rossi, G. L., and Vas, M. (2002) Nucleotide Binding to Pig Muscle 3-Phosphoglycerate Kinase in the Crystal and in Solution: Relationship between Substrate Antagonism and Interdomain Communication. *Biochemistry 41*, 111−119.
(42) Kovári, Z., Flachner, B., Náray-Szabó, G., and Vas, M. (2002) Crystallographic and thiol-reactivity studies on the complex of pig muscle phosphoglycerate kinase with ATP analogues: Correlation between nucleotide binding mode and helix flexibility. *Biochemistry 41*, 8796−8806.